



**HAL**  
open science

# Climate changes caused by degassing of sediments during the emplacement of large igneous provinces

Clément Ganino, Nicholas Arndt

► **To cite this version:**

Clément Ganino, Nicholas Arndt. Climate changes caused by degassing of sediments during the emplacement of large igneous provinces. *Geology*, 2009, 37 (4), pp.323-326. 10.1130/G25325A.1 . hal-00371235

**HAL Id: hal-00371235**

**<https://hal.science/hal-00371235>**

Submitted on 27 Mar 2009

**HAL** is a multi-disciplinary open access archive for the deposit and dissemination of scientific research documents, whether they are published or not. The documents may come from teaching and research institutions in France or abroad, or from public or private research centers.

L'archive ouverte pluridisciplinaire **HAL**, est destinée au dépôt et à la diffusion de documents scientifiques de niveau recherche, publiés ou non, émanant des établissements d'enseignement et de recherche français ou étrangers, des laboratoires publics ou privés.

# Climate changes caused by degassing of sediments during the emplacement of large igneous provinces

Clément Ganino and Nicholas T. Arndt

Laboratoire de Géodynamique des Chaînes Alpines, Université Joseph Fourier de Grenoble, CNRS, 1381 rue de la piscine 38400 Saint Martin d'Hères, France

Corresponding author: clement.ganino@ujf-grenoble.fr

## Abstract

Most mass extinctions during the last 500 m.y. coincide with eruptions of large igneous provinces (LIP): the Cretaceous-Tertiary extinction was synchronous with the Deccan flood volcanism, Permian-Triassic extinction with the eruption of the enormous Siberian Traps, and End-Guadalupian extinction with the Emeishan volcanic province. The causal link remains disputed, however, and many LIPs apparently had no significant impact on the biosphere. Here we show that a key control on the destructive consequences of LIP emplacement is the type of sedimentary rock in basins beneath the flood basalts. Contact metamorphism around intrusions in dolomite, evaporite, coal or organic-rich shale generates large quantities of greenhouse and toxic gases (CO<sub>2</sub>, CH<sub>4</sub>, SO<sub>2</sub>) which subsequently vent to the atmosphere and cause global warming and mass extinctions. The release of sediment-derived gases had a far greater impact on the environment than the emission of magmatic gases.

*Keywords: large igneous province, mass extinction, contact metamorphism, sedimentary wall-rock, Emeishan*

## Introduction

During a mass extinction, taxa from a broad range of habitats and from throughout the world disappear within a geologically brief interval (~1Ma) (Hallam and Wignall, 1997). Vogt (1972) noted that the end-Cretaceous mass extinction was synchronous with eruption of the Deccan Traps flood basalts and Courtillot and Renne (2003) have catalogued many other coincidences between mass extinction and flood volcanism. In early papers the extinctions were attributed to poisoning (Vogt 1972), global warming (Jenkyns 1999) or global cooling (Budyko and Pivivariva, 1967; Axelrod, 1981) caused by the emission of volcanic gases. A problem with this interpretation is the absence of a good correlation between the volume of erupted basalt and the impact on the biosphere, as shown in Fig. 1. The eruption of the Siberian and Emeishan basalts coincide with major extinction but the Karoo basalts, for example, can be linked only to a period of global warming (McElwain et al., 1999). Nor does the latitude at the time of eruption, which influences the efficiency of atmospheric distribution of emitted gases and aerosols, correlate with the intensity of the environmental crisis.

Here we develop the ideas of Svensen et al. (2004, 2007) and Retallack and Jahren (2008) and propose that the intensity of global climate changes may be related to the type of rocks invaded by subvolcanic intrusive complexes, rather than to the volume or nature of the degassing lava. We present new data from contact aureoles surrounding intrusions of the Emeishan province in China, a province that coincides with the major

46 end-Guadalupian environmental crisis, and we link the environmental change to  
47 massive release of CO<sub>2</sub> from the dolomites and organic-rich carbonates of the  
48 underlying sedimentary basin. We contrast this setting with the more benign effects of  
49 other LIPs which were emplaced upon older basalts, crystalline basement or  
50 sedimentary rocks low in carbon and sulfur.  
51

## 52 ***How do LIPs change the climate and cause mass extinctions?***

53 Major volcanic eruptions impact the environment in many ways: ash and sulphuric  
54 acid aerosols lead to cooling, greenhouse gases like CO<sub>2</sub>, CH<sub>4</sub> cause global warming;  
55 SO<sub>2</sub> causes acid rain; F and other halogens poison plants and animals (see Thordarson  
56 et al., 1996; Wignall, 2001 for a review). In all the LIPs shown in Figure 1, the  
57 dominant magma is tholeiitic basalt which contains relatively low contents of magmatic  
58 gases. Caldeira and Rampino (1990) estimated that the preruptive CO<sub>2</sub> concentration of  
59 the Deccan magmas (~0.2 wt%) was sufficient to cause only modest global warming;  
60 Self et al. (2006) confirmed that the mass of volcanic CO<sub>2</sub> was small compared with the  
61 CO<sub>2</sub> already present in the atmosphere and they suggested that climate perturbations  
62 were related to the emission of volcanic SO<sub>2</sub>.

63 Many LIPs also contain minor alkalic magmas, volatile-rich magmas that may have  
64 released larger quantities of volcanic gases, but there is little evidence that those  
65 provinces with higher-than-normal alkali magma contents (e.g. Ethiopia) had a  
66 disproportionate environmental impact (Courtilot and Renne, 2003). For reasons such  
67 as these we explore the hypothesis that the killer mechanism that drives global warming  
68 and mass extinctions is to be found in the sedimentary horizons beneath the flood  
69 basalts.

## 70 ***A case study: sediment degassing during the emplacement of*** 71 ***the Emeishan LIP***

72 The current, post-erosional exposure the Emeishan LIP in SW China is relatively  
73 small but the volcanic province may initially have covered >0.5 Mkm<sup>2</sup> (Courtilot and  
74 Renne 2003). Its emplacement coincides with (1) a major sea-level fall (Hallam and  
75 Wignall, 1999), (2) a negative <sup>13</sup>C excursion (Retallack et al., 2006) and (3) the major  
76 end-Guadalupian biological crisis when ~35% of all genera became extinct (Bowring et  
77 al., 1998, Zhou et al., 2002). Magmas of the Emeishan LIP intruded Proterozoic to  
78 Silurian dolostones, marls and shales of the Sichuan Basin.

79 Ganino et al. (2008) showed that the ~2000-m thick Panzhihua gabbroic sill, one of  
80 many in the Emeishan province, developed a 300 m-thick contact aureole as it intruded  
81 Proterozoic dolomites. The dominant rock type in the aureole is marble containing  
82 about 30% brucite, the hydration product of periclase. The latter mineral formed during  
83 prograde metamorphism of dolomite, a process that yields abundant CO<sub>2</sub>. The trace  
84 element composition of a brucite marble immediately adjacent to the intrusive contact  
85 shows evidence of partial melting of carbonates; farther from the contact,  
86 metamorphism of impure limestones formed calc-silicates. Both processes released  
87 additional CO<sub>2</sub>. Several hundred kilometres to the north-west of the Emeishan basalts,  
88 shales and limestones of the Sichuan Basin contain gas and petroleum deposits (Wei et  
89 al., 2008) and the metamorphism of hydrocarbons in contact aureoles may have  
90 released CO<sub>2</sub> and CH<sub>4</sub>. In the following section we quantify the amounts of CO<sub>2</sub>  
91 released from magmatic and sedimentary sources.  
92

## 93 **Quantification of gas release during emplacement of the** 94 **Panzhihua intrusion**

95 Following Self et al.'s (2006) estimation of CO<sub>2</sub> release from Deccan volcanism,  
96 we estimate that ~2 Gt of magmatic CO<sub>2</sub> (= 0.55 Gt C) was released from the 180 km<sup>3</sup>  
97 of magma in the Panzhihua intrusion.

98 Three main reactions took place during the metamorphism of Panzhihua wall rocks,  
99 depending on the temperature. We first focus on the intermediate-temperature  
100 periclase-forming reaction dolomite = periclase + calcite + CO<sub>2</sub>. From the reaction we  
101 calculate that 240 g of CO<sub>2</sub> are released per kilogram of dolomite. From the dimensions  
102 of the lower contact aureole (19 km long, 300 m wide and an assumed 3 km in depth),  
103 we calculate its mass as ~ 47 Gt (density = 2700 kg.m<sup>-3</sup>) to give a total of 11.2 Gt of  
104 CO<sub>2</sub> (or 3.1 Gt C). An equivalent mass of CO<sub>2</sub> probably was released by periclase  
105 formation in an upper contact aureole, which is not preserved due to faulting.

106 We can use the presence of periclase, which formed at 700°C in samples collected  
107 300 m from the intrusive contact, to define the temperature profile in the aureole (Fig.  
108 2). We modelled the development of the aureole assuming that basaltic magma  
109 continuously flowed through the sill to maintain a temperature of 1200°C at the contact.  
110 In a simple conductive model, the profile requires 2500 years to form; when fluid  
111 advection is taken into account, the time is shorter. Such a temperature profile explains  
112 the presence of melted carbonates adjacent to the intrusion (~1200°C) and the presence  
113 of periclase, which forms at ~700°C at a depth 300 m below the lower contact.

114 We now use this profile to estimate the quantities of gas released by high- and low-  
115 temperature reactions (see supplementary material). The calculation is only  
116 approximate because we have relatively little information about the exact geometry and  
117 structure of the contact aureole, but it is sufficient to provide a first-order estimate.  
118 High-temperature reactions such as the assimilation and partial melting of dolostone  
119 yield abundant CO<sub>2</sub> but only within a few metres of the contact. An indication of the  
120 amount of CO<sub>2</sub> that might be released by the assimilation of wall-rock in mafic magmas  
121 is provided by Iacono Marziano et al. (2007) who calculated that lavas of Mt Vesuvius  
122 had assimilated 15-17 wt% of limestone.

123 Calc-silicates form from impure marble between 450 and 500°C and these reactions  
124 release between 220 and 290 g per kg of rock. Total degradation of hydrocarbons at  
125 temperatures above 300°C would have released additional methane and CO<sub>2</sub>. The large  
126 range of concentration and maturation of organic carbon, preclude any precise  
127 quantification of the mass of CO<sub>2</sub> released during low temperature degradation of  
128 hydrocarbon, but some limits can be calculated. If the wall rocks contained a low  
129 content of organic carbon (0.01 wt%) the input (0.02 Gt C) would be negligible but if  
130 they contained 4 wt% organic carbon, as observed in source rock of the Sichuan Basin  
131 (Wei et al., 2008), then the mass of CO<sub>2</sub> would be 8.1 Gt C, similar to that released  
132 from the periclase reaction.

133 Given these results, we estimate that a total of at least 22 Gt of CO<sub>2</sub> from the  
134 periclase reaction, and up to ~52 Gt equivalent CO<sub>2</sub> (=14.1 Gt C) if the wall-rock  
135 contained large amount of organic carbon, was formed from the contact aureoles. These  
136 values can be compared with the ~2 Gt CO<sub>2</sub> (=0.54 Gt C) released from the magma. At  
137 the intrusion scale, the mass of sediment-derived carbon is some 11 to 26 times greater  
138 than the mass of magmatic carbon.

### 139 **Gas-release during the Emeishan LIP at the basin scale**

140 Because of intense Himalaya-related deformation it is difficult to estimate the total  
141 amount of sedimentary rock of the Sichuan Basin that was affected by metamorphism.  
142 Taking as a model the better-preserved lava piles and sedimentary basins in the  
143 Siberian and Karoo volcanic provinces (Czamanske et al., 2002; Chevallier and  
144 Woodford, 1999), we assume that about half of the volume of the Emeishan volcanic  
145 pile was emplaced as shallow-level intrusions. Courtillot and Renne (2002) calculate  
146 that the total volume of the erupted basalt in the Emeishan LIP was  $\sim 1 \text{ Mkm}^3$  and,  
147 following Self et al.'s (2006) estimation for the Deccan, such a volume of magma  
148 would release 11 200 Gt of  $\text{CO}_2$  (= 3057 Gt C). Magma in intrusions emitted an  
149 additional 5600 Gt of  $\text{CO}_2$  bringing the total to 16800 Gt of  $\text{CO}_2$  or 4585 Gt of C.

150 If the Panzihua intrusion is representative of an average sill in the intrusive  
151 complex below the lava pile, 11 to 26 times more metamorphic  $\text{CO}_2$  ( $5600 \times 11 = 61600$   
152  $5600 \times 26 = 145600$  Gt  $\text{CO}_2$ ) was released from contact aureoles. Thus at the LIP scale,  
153 the mass of sediment-derived  $\text{CO}_2$  is about 3.6 to 8.6 times larger than the mass of  
154 magmatic  $\text{CO}_2$ .

155

### 156 **Proxies of climate change in Emeishan-age sediments**

157 Can  $\text{CO}_2$  released during contact metamorphism of carbonates explain the negative  
158 carbon isotope excursion at the end-Guadalupian which is recorded in both marine  
159 carbonate and continental organic matter by Retallack et al. (2006)? During the end-  
160 Guadalupian, the  $\delta^{13}\text{C}$  of marine carbonates decreased from about +3 to -2 ‰, and that  
161 of nonmarine clastic organic carbon from about -22 to -30 ‰ (Retallack et al., 2006). If  
162 we suppose that 17000 Gt C from the destabilisation of dolostone (with  $\delta^{13}\text{C} = 0$ ) and  
163 22900 Gt C from the metamorphism of organic carbon (with  $\delta^{13}\text{C} \sim -22$ ) were added to  
164 the ocean-atmosphere, a global negative carbon isotope excursion would result (see  
165 supplementary material for details). Atmospheric carbon composition would change  
166 from  $\delta^{13}\text{C} = -2$  before the degassing to as low as -10.9 after the degassing.

167 There are few reliable proxies for the climate changes during the emplacement of the  
168 Emeishan LIP.

### 169 **Sediment degassing and mass extinctions**

170 Figure 2 is a synthesis of the total amount of volatiles released during the contact  
171 metamorphism of different types of sedimentary rocks. The inputs that must be  
172 considered when evaluating the environment impact of LIP emplacement can be  
173 summarized as follows:

- 174 • Basalt and granitoids do not release abundant volatiles.
- 175 • In most sandstones, the main volatile is water whose release has little effect on  
176 global climate.
- 177 • Pure limestone contains large amounts of  $\text{CO}_2$  but the thermal decomposition of  
178 limestone into  $\text{CaO}$  and  $\text{CO}_2$  takes place at high temperatures ( $>950^\circ\text{C}$ ) that are rarely  
179 reached in contact aureoles.
- 180 • Impure limestones release large amounts of  $\text{CO}_2$  (up to 29 wt%) during the  
181 formation of calc-silicates at moderate temperatures of  $\sim 450$  to  $500^\circ\text{C}$ .
- 182 • Gypsum and anhydrite in evaporites release abundant  $\text{SO}_2$  (up to 47%). This  
183 reaction normally happens at high temperatures ( $1400^\circ\text{C}$ ) that are not observed in  
184 contact aureoles, but the reaction proceeds at temperature as low as  $615^\circ\text{C}$  for impure  
185 anhydrite (West and Sutton, 1954).
- 186 • Contact metamorphism of salt releases halocarbons.

- 187 • Sulfidic sediments release abundant SO<sub>2</sub> at low temperature.
- 188 • Organic carbon-rich shales and carbonates release methane and hydrocarbon
- 189 when heated at relatively low temperature (<300°C).
- 190 • Coal releases abundant CO<sub>2</sub> if ignited.

191

192 Figure 1 shows that there is no clear link between volume of the LIP and magnitude of  
193 mass extinction. Degassing of magmatic volatiles therefore cannot be the sole cause of  
194 the environmental changes and mass extinctions and gas release from sediments may be  
195 implicated in various ways:

196 1. The Ontong-Java oceanic plateau, the largest magmatic province, formed in a  
197 submarine volcanic setting and is not associated with a large mass extinction. The  
198 dominant wall rock is basalt which yields no toxic or greenhouse gases (dehydration of  
199 altered basalt has little climatic impact). Eruption into water may have restricted release  
200 of gas into the atmosphere.

201 2. Emplacement of the Deccan traps coincides with the K-T mass extinction (e.g.  
202 Courtillot and Renne, 2002). Here the substrate consists of minor clastic sediments and  
203 crystalline basement, which do not yield additional volatiles, and a combination of  
204 Chixculub meteorite impact (e.g., Alvarez et al. 1980) and the release of magmatic  
205 gases (Chenet et al., 2008) may account for the K-T mass extinction.

206 3. Eruption of the Siberian traps, the largest continental flood basalt province,  
207 coincided with the largest known mass extinction. The volume of basalt cannot explain  
208 the intensity of the crisis by itself. Intrusions beneath the Siberian traps invaded marls,  
209 limestones, sandstones, coal and most significantly, evaporites (Czamanske et al.,  
210 2002). The sulphur isotope signature of sulfide ores provides evidence that sulfur from  
211 evaporites was assimilated into magma (Ripley et al., 2003). Part of the sulfur  
212 contained in the magma was probably released as SO<sub>2</sub> during the eruption, and  
213 additional SO<sub>2</sub>, CO<sub>2</sub>, the breakdown products of hydrocarbons, would be expelled from  
214 the contact aureoles (Retallack and Jahren, 2008). Global dispersion of SO<sub>2</sub> from  
215 Siberian traps volcanism was aided by the high latitude of these eruptions (e.g.,  
216 Saunders, 2005).

217 4. The Emeishan plateau erupted at equatorial latitude and here the consequences  
218 were different. The dispersion of CO<sub>2</sub> is largely independent of latitude because of the  
219 high exchange rate between the stratosphere and the troposphere. We suggest therefore  
220 that the coincidence between the Emeishan volcanism and the end-Guadalupian crisis  
221 can be explained by the voluminous release of CO<sub>2</sub> from the heating of dolomite  
222 augmented by CO<sub>2</sub>, SO<sub>2</sub> and CH<sub>4</sub> from evaporites and shales.

223 In those provinces where the environmental impact was minor, the wall rocks were  
224 sandstone, organic-poor shales or granitic basement. Svensen et al. (2007) estimated  
225 that up to 27400 Gt may have formed during contact metamorphism of shales and  
226 sandstones of the Karoo basin, enough to explain the Early Jurassic global warming but  
227 not sufficient to cause a mass extinction. Likewise, the Central Atlantic Magmatic  
228 Province coincides with the Triassic-Jurassic mass extinction but the influence of this  
229 very large province may have been mitigated by the largely crystalline nature of its wall  
230 rocks

## 231 **Conclusion**

232 Sedimentary rocks are huge reservoirs of volatiles that are readily released by contact  
233 metamorphism. The degassing associated with contact metamorphism is much more  
234 voluminous than the degassing of the magma itself. We have identified two major  
235 mechanisms responsible for large gas emissions and mass extinctions: (1) the

236 destabilization of dolomite, which caused massive CO<sub>2</sub> release during the emplacement  
237 of Emeishan and other LIPs, (2) the thermal decomposition of anhydrite, salt,  
238 limestone, hydrocarbons and coal in other provinces, which provided a toxic cocktail  
239 that caused other mass extinctions. Other provinces were emplaced in sterile magmatic  
240 or sedimentary rocks and had little to no environmental impact.

241

## 242 **Acknowledgements**

243 We express our gratitude to Henrik Svensen for his constructive comments and his help  
244 with the preparation of the manuscript. We also thank Catherine Chauvel, Fernando  
245 Tornos, Lukas Baumgartner and Didier Marquer for constructive discussions; Mei-Fu  
246 Zhou and Yuxiao Ma for assistance during our field work; and Chris Harris for  
247 providing stable isotope analyses. The project was supported by two Egide exchange  
248 programs PROCORE (France Hong Kong) and Aurora (France-Norway). Further  
249 support was obtained from the French CNRS (DyETI program).

250

## 251 **References cited**

252 Alvarez, L.W., Alvarez, W., Asaro, F., and Michel, H.V., 1980. Extraterrestrial cause  
253 for the Cretaceous Tertiary extinction: *Science*, v. 208, p. 1095–1108, doi:  
254 10.1126/science.208.4448.1095.

255 Axelrod, D.I., 1981. Role of volcanism in climate and evolution: *Geol. Soc. Am., Spec.*  
256 *Pap.* 185, 1–59.

257 Bowring, S.A., Erwin, D.H., Jin, Y.G., Martin, M.W., Davidek, K., and Wang W.,  
258 1998, U/Pb Zircon Geochronology and Tempo of the End-Permian Mass  
259 Extinction: *Science*, v. 280, p. 1039-1045, doi: 10.1126/science.280.5366.1039.

260 Budyko, M.I., and Pivivariva, Z.I., 1967, The influence of volcanic eruptions on solar  
261 radiation incoming to the Earth's surface: *Meteorol. Gidrol.*, v. 10, p. 3–7.

262 Caldeira, K., and Rampino, M.R., (1990), Carbon dioxide emissions from Deccan  
263 volcanism and a K/T boundary greenhouse effect: *Geophysical Research*  
264 *Letters*, v. 17, p. 1299–1302.

265 Chenet, A.L., Fluteau, F., Courtillot, V., Gérard, M., and Subbarao, K.V., 2008,  
266 Determination of rapid Deccan eruptions across the Cretaceous-Tertiary  
267 boundary using paleomagnetic secular variation: Results from a 1200-m-thick  
268 section in the Mahabaleshwar escarpment: *Journal of Geophysical Research*  
269 v.113, B04101, doi: 10.1029/2006JB004635.

270 Chevallier, L., and Woodford, A., 1999, Morpho-tectonics and mechanism of  
271 emplacement of the dolerite rings and sills of the western Karoo, South Africa:  
272 *South African Journal of Geology*, v. 102, p. 43-54.

273 Courtillot, V., and Renne, P.R., 2003, On the ages of flood basalt events: *Comptes*  
274 *Rendus Geoscience*, v. 335, p. 113-140, doi: 10.1016/S1631-0713(03)00006-3.

275 Czamanske, G.K., Zen'ko, T.E., Fedorenko, V.A., Calk, L.C., Budahn, J.R., Bullock,  
276 J.H., Fries, T., King, B.-S., and Siems, D., 2002, Petrographic and geochemical  
277 characterization of ore-bearing intrusions of the Noril'sk type. Siberia: With  
278 discussion of their origin, including additional datasets and core logs: *US*  
279 *Geological Survey Open-File Report*: 02-74.

280 Ganino, C., Arndt, N.T., Zhou, M.F., Gaillard, F., and Chauvel, C., 2008, Interaction of  
281 magma with sedimentary wall rock and magnetite ore genesis in the Panzhihua  
282 mafic intrusion, SW China, *Mineralium deposita*, 43, 677-694, doi:  
283 10.1007/s00126-008-0191-5.

- 284 Hallam, A. and Wignall, P.G., 1997, *Mass Extinctions and Their Aftermath*: Oxford  
285 University Press, 334 p.
- 286 Hallam, A. and Wignall, P.B., 1999, Mass extinctions and sea-level changes: *Earth-*  
287 *Science Reviews*, v. 48, p. 217–250, doi: 10.1016/S0012-8252(99)00055-0.
- 288 Iacono Marziano, G., Gaillard, F., and Pichavant, M., 2007, Limestone assimilation by  
289 basaltic magmas: an experimental re-assessment and application to Italian  
290 volcanoes: *Contributions to Mineralogy and Petrology*, v. 154, p. 1-20, doi:  
291 10.1007/s00410-007-0267-8.
- 292 Jenkyns, H.C., 1999, Mesozoic anoxic events and palaeoclimate: *Zentralblatt für*  
293 *Geologie und Paläontologie*, p. 943–949.
- 294 McElwain, J.C., Beerling, D.J., and Woodward, F.I., 1999, Fossil Plants and Global  
295 Warming at the Triassic-Jurassic Boundary: *Science*, v. 285, p. 1386-1390, doi:  
296 10.1126/science.285.5432.1386.
- 297 Retallack, G.J., Metzger, C.A., Greaver, T., Jahren, A.H., Smith, R.M.H., and Sheldon,  
298 N.D., 2006, Middle-Late Permian mass extinction on land: *Bulletin of the*  
299 *Geological Society of America*, v. 118, p. 1398-1411, doi: 10.1130/B26011.1.
- 300 Retallack, G.J., and Jahren, A.H., 2008, Methane release from igneous intrusion of coal  
301 during late Permian extinction events: *The Journal of Geology*, v. 116, p. 1-20,  
302 doi: 10.1086/524120.
- 303 Ripley, E.M., Lightfoot, P.C., Li, C., and Elswick, E.R., 2003, Sulfur isotopic studies of  
304 continental flood basalts in the Noril'sk region: implications for the association  
305 between lavas and ore-bearing intrusions: *Geochimica et Cosmochimica Acta*,  
306 v. 67, p. 2805-2817, doi:10.1016/S0016-7037(03)00102-9.
- 307 Rohde, R.A., and Muller, R.A., 2005, Cycles in fossil diversity: *Nature* v. 434, p. 208-  
308 210, doi: 10.1038/nature03339.
- 309 Saunders, A.D., 2005, Large Igneous Provinces: Origin and Environmental  
310 Consequences: *Elements*, v. 1, p. 259-263, doi: 10.2113/gselements.1.5.259.
- 311 Self, S., Widdowson, M., Thordarson, T., and Jay A.E., 2006, Volatile fluxes during  
312 flood basalt eruptions and potential effects on the global environment: A Deccan  
313 perspective: *Earth and Planetary Science Letters*, v. 248, p. 518-532,  
314 doi:10.1016/j.epsl.2006.05.041.
- 315 Svensen, H., Planke, S., Malthe-Sørensen, A., Jamtveit, B., Myklebust, R., Eidem, T.,  
316 and Rey, S.S., 2004, Release of methane from a volcanic basin as a mechanism  
317 for initial Eocene global warming: *Nature*, v. 429, p. 542-545, doi:  
318 10.1038/nature02566.
- 319 Svensen, H., Planke, S., Chevallier, L., Malthe-Sørensen, A., Corfu, B., and Jamtveit,  
320 B., 2007, Hydrothermal venting of greenhouse gases triggering Early Jurassic  
321 global warming: *Earth and Planetary Science Letters*, v. 256, p. 554-566, doi:  
322 10.1016/j.epsl.2007.02.013.
- 323 Thordarson, T., Self, S., Óskarsson, N., and Hulsebosch, T., 1996, Sulfur, chlorine, and  
324 fluorine degassing and atmospheric loading by the 1783-1784 AD Laki (Skaftár  
325 Fires) eruption in Iceland: *Bulletin of Volcanology*, v. 58, p. 205-225,  
326 doi:10.1007/s004450050136.
- 327 Vogt, P.R., 1972, Evidence for global synchronism in mantle plume convection, and  
328 possible significance for geology: *Nature*, v. 240, p. 338-342, doi:  
329 10.1038/240338a0.
- 330 Wei, G., Chen, G., Du, S., Zhang, L., and Yang, W., 2008, Petroleum systems of the  
331 oldest gas field in China: Neoproterozoic gas pools in the Weiyuan gas field,  
332 Sichuan Basin: *Marine and Petroleum Geology*, v. 25, p. 371-386, doi:  
333 10.1016/j.marpetgeo.2008.01.009.



- 334 West, R.R. and Sutton W.J., 1954, Thermography of Gypsum: Trans. Central Geol.  
335 Prospecting Znst (USSK), v. 88, p. 1-66.
- 336 Wignall, P.B., 2001, Large igneous provinces and mass extinctions: Earth-Science  
337 Reviews, v. 53, p. 1–33, doi: 10.1016/S0012-8252(00)00037-4.
- 338 Zhou, M.-F., Malpas, J., Song, X.-Y., Robinson, P.T., Sun, M., Kennedy, A.K., Lesher,  
339 C.M., and Keays, R.R., 2002, A temporal link between the Emeishan large  
340 igneous province (SW China) and the end-Guadalupian mass extinction: Earth  
341 and Planetary Science Letters, v. 196, p. 113-122, doi: 10.1016/S0012-  
342 821X(01)00608-2.
- 343
- 344

345 Figure captions

346

347 **Fig 1. Volume of erupted basalt from Courtillot and Renne (2003) vs percentage of**  
348 **generic extinctions (from *Rhodes and Muller 2005*) for major LIPs. Two main**  
349 **populations of LIPs are evident, one for which the associated rate of extinction is**  
350 **close to the background rate (Columbia River to Ontong Java) and another for**  
351 **which the rate is far higher. Those in the latter group intrude sedimentary rocks**  
352 **that released abundant greenhouse or toxic gases.**

353

354

355 **Fig 2. Theoretical thermal profile in a Panzhihua-like contact aureole. The**  
356 **horizontal bars indicate the maximum distance into the aureole where the**  
357 **metamorphic reactions take place. The black portion of each bar represents the**  
358 **proportion of gas released by the reaction.**

359

360

Fig. 1

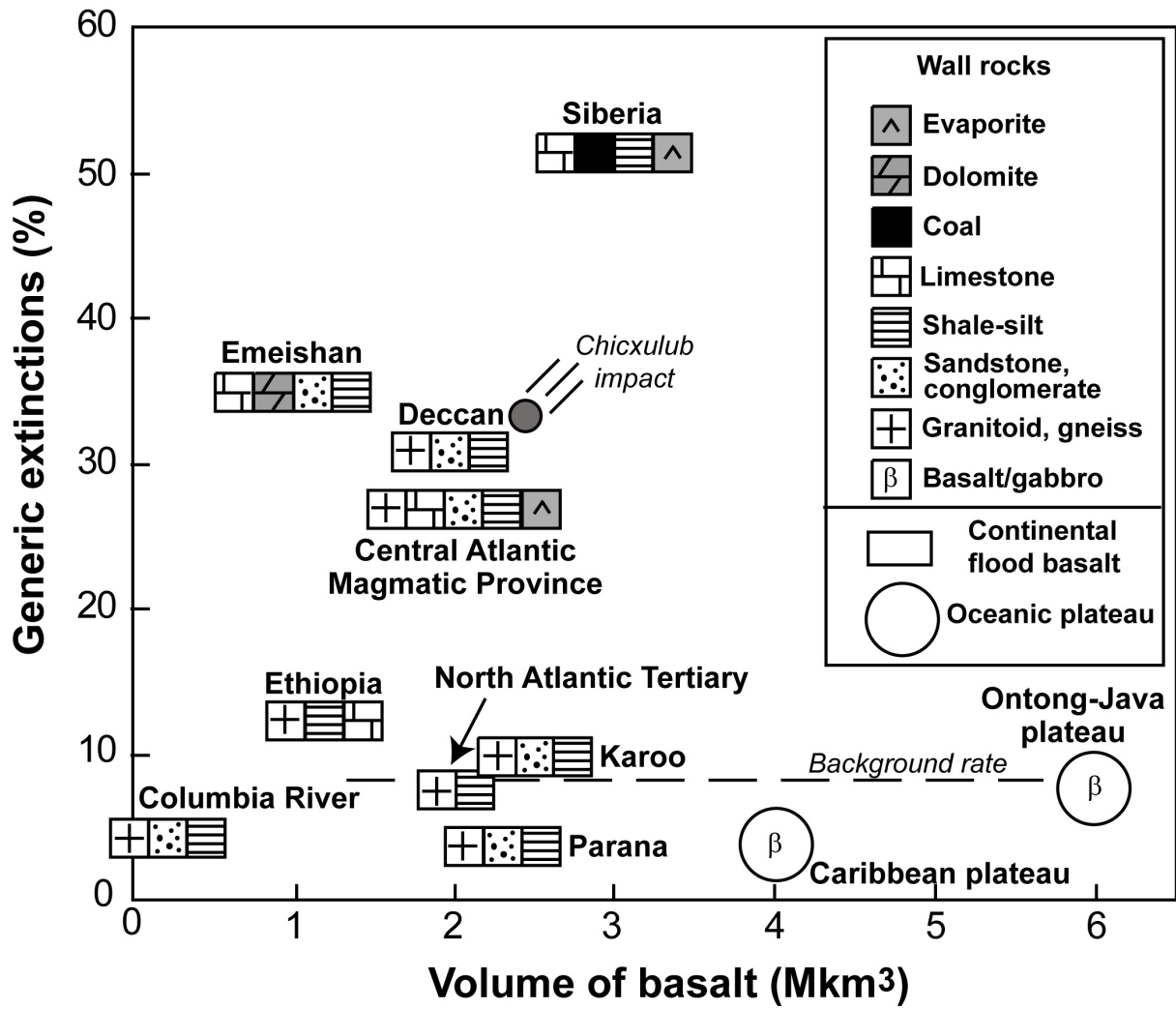
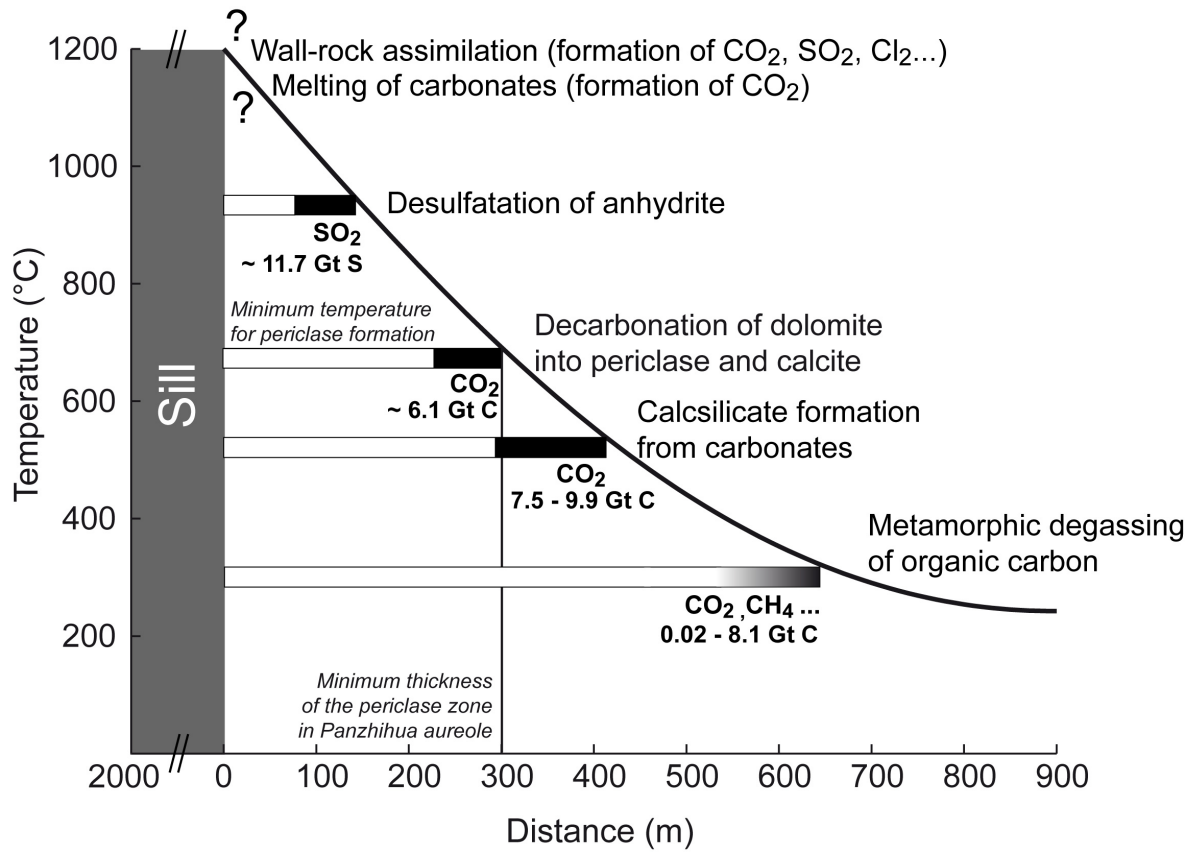


Fig.2



362  
363  
364 |

365 **Supplementary material 1: Degassing during contact metamorphism as**  
366 **an explanation of the negative carbon isotope excursion associated with**  
367 **the emplacement of the Emeishan LIP**  
368

369 Our measurements of the  $\delta^{13}\text{C}$  of dolostones from the Sinian formation range from +4.7  
370 to -1.1, values which are consistent with Jacobsen and Kaufman's (1998) estimate of  
371  $\delta^{13}\text{C}$  in Neoproterozoic seawater (+4 to -4 ‰, with most of the data between +2 and -2  
372 ‰). If we assume that (1) end-Guadalupian seawater contained ~40000 Gt C with  $\delta^{13}\text{C}$   
373 = +5 ‰ (Berner, 2005), (2) end-Guadalupian atmosphere contained ~2850 Gt C  
374 (Rothman 2002) with  $\delta^{13}\text{C}$  = -2 ‰ (7 ‰ more negative than seawater (Mora et al.  
375 1996)), then the average  $\delta^{13}\text{C}$  of the ocean-atmosphere system was +4.5.

376 After the addition of 16800 Gt of magmatic  $\text{CO}_2$  (4580 Gt C with  $\delta^{13}\text{C}$  = -6),  
377 62500 Gt of  $\text{CO}_2$  from destabilized Sinian dolostone (17000 Gt C with  $\delta^{13}\text{C}$  = 0) and  
378 potentially 84000 Gt  $\text{CO}_2$  from the metamorphism of organic carbon (=22900 Gt C  
379 with  $\delta^{13}\text{C}$  ~ -22), the bulk composition of the ocean-atmosphere system is changed to  
380 between  $\delta^{13}\text{C}$  = +2.6 ‰ (if no organic contribution) and -3.9 (if 22900 Gt C from the  
381 metamorphism of organic carbon was added with  $\delta^{13}\text{C}$  ~ -22). If we then assume that  
382 ocean-atmosphere equilibrium is rapid (flux ~90 Gt/y as current estimation) and the  
383 difference between the carbon isotope compositions of ocean and atmosphere is fixed at  
384 the timescales we consider ( $\delta^{13}\text{C}_{\text{atm}} = \delta^{13}\text{C}_{\text{ocean}} - 7$  ‰), as supposed by Mora (1996) and  
385 Beerling et al. (2002), then the effect of emplacement of the Emeishan LIP in the Sinian  
386 Basin is a negative carbon excursion for the ocean-atmosphere system from an average  
387 of  $\delta^{13}\text{C}$  = -2 before the degassing to an average of  $\delta^{13}\text{C}$  = -4.4 to -10.9 after degassing.  
388

389 References cited

- 390 Beerling, D.J., Lake, J.A., Berner, R.A., Hickey, L.J., Taylor D.W., and Royer D.L.,  
391 2002, Carbon isotope evidence implying high  $\text{O}_2/\text{CO}_2$  ratios in the Permo-  
392 Carboniferous atmosphere. *Geochimica et Cosmochimica Acta*, v. 66, p. 3757-  
393 3767, doi: 10.1016/S0016-7037(02)00901-8.
- 394 Berner, R.A., 2005, The carbon and sulphur cycles and atmospheric oxygen from  
395 middle Permian to middle Triassic: *Geochimica et Cosmochimica Acta*, v. 69,p.  
396 3211-3217, doi: 10.1016/j.gca.2005.03.021.
- 397 Jacobsen, S.B., and Kaufman, A.J., 1999, The Sr, C and O isotopic evolution of  
398 Neoproterozoic seawater: *Chemical Geology*, v. 161, p. 37-57, doi:  
399 10.1016/S0009-2541(99)00080-7.
- 400 Mora, C.I., Driese, S.G., and Colarusso, L.A., 1996, Middle to Late Paleozoic  
401 Atmospheric  $\text{CO}_2$  Levels from Soil Carbonate and Organic Matter: *Science*, v.  
402 271, p. 1105-1107, doi: 10.1126/science.271.5252.1105.

403

404 |

405

406 **Supplementary material 2: An overview of reactions in a metamorphic**  
407 **aureole in a sedimentary basin**

408 The amount of gas released during metamorphism depends on the type of sediment and  
409 its chemical composition, and on the conditions (P,T, Xfluid) of metamorphism.

- 410 • At the highest temperatures, calcite melts incongruently to CaO and CO<sub>2</sub>. Solid or  
411 liquid calcite is assimilated into the magma where it reacts to Ca which is absorbed  
412 in the magma or overlying rocks and CO<sub>2</sub>, which degasses.
- 413 • Thermal decomposition of pure anhydrite ( $\text{CaSO}_4 = \text{CaO} + \text{SO}_2 + \frac{1}{2} \text{O}_2$ ) begins at  
414 1100°C and reacts readily only at temperatures around 1400 °C. Impure anhydrite  
415 containing clay, graphite or carbon monoxide reacts at temperatures well below  
416 1000°C ( $2\text{CaSO}_4 + \text{C} = 2\text{CaO} + \text{CO}_2 + 2\text{SO}_2$  and  $\text{CaSO}_4 + \text{CO} = \text{CaO} + \text{CO}_2 +$   
417  $\text{SO}_2$ ). Kuusik et al. (1985) report thermal decomposition of anhydrite in CO/N  
418 mixtures at 900 °C. Impurities such as SiO<sub>2</sub> lower the decomposition temperatures  
419 by up to 100 °C. West and Sutton (1954) report decomposition of anhydrite with  
420 20% added carbon at 615°C in a nitrogen atmosphere.
- 421 • Thermal decomposition of pure limestone ( $\text{CaCO}_3 = \text{CaO} + \text{CO}_2$ ) strongly depends  
422 on the water content. In the absence of water, decomposition starts only at high  
423 temperature, around 1200°C; when aqueous fluid is present, the temperature is  
424 lower (~700°C).
- 425 • Dolomite reacts to calcite, periclase and CO<sub>2</sub> ( $\text{CaMg}(\text{CO}_3)_2 = \text{CaCO}_3 + \text{MgO} +$   
426  $\text{CO}_2$ ) at 700°C. In the presence of aqueous fluid the temperature decreases to below  
427 ~450°C
- 428 • Calc-silicates containing forsterite and diopside form from impure limestones and  
429 marls. These reactions release considerable CO<sub>2</sub> and proceed at relatively low  
430 temperatures, between 450 and 500°C.
- 431 • Organic matter in carbonates or shales releases CH<sub>4</sub> and/or CO<sub>2</sub>. Cracking of  
432 hydrocarbons starts at ~100°C and reaches a maximum around 550 °C.
- 433 • Other gases are released from specific sediment types. Salts break down to  
434 halogens; pyrite in sulfide-rich shales oxidises or breaks down to Fe-oxide releasing  
435 sulfur oxides; coal burns to release CO<sub>2</sub>.

436 The reactions within an aureole thus release a series of greenhouse or toxic gases,  
437 including CO<sub>2</sub>, SO<sub>2</sub>, CH<sub>4</sub>, and halogens, as summarized in Figure 2.

438

439 **References cited**

440 Kuusik, R., Saikkonen, P., and Niinisto, L., 1985, Thermal decomposition of calcium  
441 sulfate in carbon monoxide: Journal Thermal Analysis and Calorimetry, v. 30,  
442 p. 187-193.

443

444

445

446